Eur. Phys. J. B (2012) 85: 329
DOI: 10.1140/epjb/e2012-30471-9

THE EUROPEAN PHYSICAL JOURNAL B

Colloquium

Current challenges for statistical physics in fracture and plasticity

S. Zapperi[a]

CNR – Consiglio Nazionale delle Ricerche, IENI, Via R. Cozzi 53, 20125 Milano, Italy
ISI Foundation, Via Alassio 11C, 10133 Torino, Italy

Received 13 June 2012
Published online 24 September 2012 –

Abstract. Statistical physics has been applied in the last decades to several problems in mechanics, including fracture and plasticity. Concept drawn from percolation, fractal geometry, phase-transitions, and interface depinning have been used with varying degrees of success to understand these problems. In this colloquium, I describe recent successes and current challenging problems for statistical physics in fracture and plasticity, focusing on the roughness of cracks, fracture size effects and micron-scale plasticity.

1 Introduction

Understanding how materials respond to external mechanical perturbations is a central problem of science and engineering. In most practical cases disorder and fluctuations are unavoidable, leading to sample-to-sample variations and non-trivial size effects. The size dependence of strength is a well known but still unresolved issue in the context of fracture (for a recent review see [1]). Similarly, in micro and nanoscale samples, the plastic yield strength displays size effects and strain bursts [2,3], features that are not present in macroscopic samples where plasticity is a smooth process (for recent reviews on microplasticity see [4–6]). These problems are becoming particularly important in the current miniaturization trend towards nanoscale devices, since the relative amplitude of fluctuations grows as the sample size is reduced. The presence of large fluctuations makes the use of conventional continuum mechanics problematic and calls instead for a statistical physics approach.

Most of the complexity in fracture and plasticity stems from the interplay between long-range elastic interactions and structural disorder. Statistical physicists have developed a full machinery of analytical and numerical methods to tackle these problems. For instance, theories for the depinning transition of elastic manifolds of disordered media [7,8] play a central role in our current understanding of various problems, from crack propagation and roughening to solid solution hardening in plastically deformed materials. Yet, a complete quantitative description is only possible for simple idealized systems like single a planar crack in a random toughness field [9–12] or individual or periodic arrays of dislocations in a cloud of immobile solute atoms or threading dislocations [13,14]. In most cases, however, fracture and plasticity are due to more complex processes in which many interacting cracks or dislocations grows or move at the same time. It is an open question if concepts and ideas valid idealized systems can be applied directly to more realistic conditions.

Fracture size effects are a fundamental problem in the design of components, structures and devices that are subject to elastic loads. It is clear that when we design something, we want to make sure that it does not fail afterwards. The straightforward way to avoid this problem is to perform a test and see what is the load that can be carried by our sample without failing. Then this result can be used to define appropriate safety factors for the reliability of structures, components etc. This program faces, however, two main difficulties. First, the strength is usually not a deterministic but a random variable, so that nominally identical samples can fail at very different loads. Hence, a test on on a single sample is usually not enough. Second, performing a direct test is not always feasible. The classical example is the construction of a dam: we cannot test in advance if the dam will resist a flood. What is done is to examine small scale models and then rescale the results, but this can only be done if we can adequately control size effects. Failure to do so has produced terrible catastrophes in the past, such as the collapse of the Malpasset dam in 1959 killing 400 people [15]. While our understanding of size effects has improved in the past century, with countless phenomenological theories, both statistical and deterministic, there is still no consensus in the literature about what law to use and when.

Plasticity has the convenient feature of being size independent at large scales, and therefore the design of reliable large scale structures is not such a big issue as in fracture. Size effects arising at small scales, however, may generate serious problems for plastic forming processes in materials processing and manufacturing technology. Due to the current trend in pushing devices to smaller and smaller scales, a new frontier of the field is represented by the study of micro and nanoscale plasticity – a typical application are

[a] e-mail: stefano.zapperi@cnr.it

bonding wires for connecting integrated circuits, with wire thickness that is rapidly approaching the micron range. At these scales, size independent smooth plastic flow, described by conventional continuum plasticity, gives way to scale dependent spatio-temporal intermittency and randomness. Unpredictable fluctuations in the mechanical properties and spontaneous deformation localization may reduce formability and hinder device functioning. It would be desirable to produce strong micron-sized components, with high yield stresses but without the nuisance of intermittency. At present, it is not clear if this might even be possible. These findings pose intriguing questions about the possibility of homogenization, and hence about the applicability of continuum descriptions for micron sized samples. Increasing miniaturization of mechanical devices is rapidly leading us to scales where the typical finite element mesh becomes of the order of the size of collective plastic fluctuations. In order to tackle this issue, we need to make a step backwards to the very foundations of plasticity theory.

In this colloquium, I will first discuss the problem of crack roughness, describing the success of the depinning theory and highlighting open issues. Next, I will discuss current challenges posed by size effects in fracture and micron-scale plasticity.

2 Crack roughness

2.1 Self-affine scaling of crack surfaces

Understanding the morphological properties of fracture surfaces has been a major topic of investigation in the last decades. Fracture surface have been originally characterized by self-affine scaling [16,17], but understanding the value of the roughness exponent and its universality classes is still an open problem (for a recent and comprehensive review see [18]). Crack surfaces are characterized by a height profile $h(x, y)$, where x is the direction of propagation of the crack (see Fig. 1A). Most early measurements focused on the out-of plane correlation function along the y direction,

$$C(y - y') \equiv \langle (h(x, y) - h(x, y')) \rangle \simeq |y - y'|^{2\zeta_\perp} \qquad (1)$$

with a universal exponent $\zeta_\perp \simeq 0.8$ irrespective of the material studied [17]. In particular, experiments have been done in metals [19], glass [20] and rocks [21], covering both ductile and brittle materials. Some experiments revealed a small exponent $\zeta_\perp = 0.4 - 0.6$ at smaller length scales [17]. It was originally conjectured that crack roughness displays a universal value of $\zeta_\perp \simeq 0.8$ only at larger scales and at higher crack speeds, whereas another roughness exponent in the range of $0.4 - 0.6$ would be observed at smaller length scales under quasi-static or slow crack propagation [17]. However, more recent experimental results revealed that the short-scale value is not present in silica glass, even when cracks move at extremely low velocities [22]. In addition, in sandstone and glass ceramics, it was only possible to measure a value of $\zeta_\perp \simeq 0.45$ even at high velocities [22,23].

Crack surfaces has also been analyzed along both directions, showing an anisotropic scaling behavior [22,24]

$$\Delta h(\Delta y, \Delta x) = \Delta x^{\zeta_\parallel} f(\Delta y / \Delta x^{1/z})$$
$$\text{where} \quad f(u) \sim \begin{cases} 1 & \text{if } u \ll 1 \\ u^{\zeta_\perp} & \text{if } u \gg 1. \end{cases} \qquad (2)$$

Equation (2) has the same form of Family-Vicsek scaling, with $z = \zeta_\perp / z_\parallel$ being the dynamic exponent, commonly used to describe spatio-temporal roughness of dynamics interfaces. In the case of fracture x would play the role of time. This is justified by the fact that the final fracture surface is nothing but the trail left by the crack line as it advances through the medium [20,25].

2.2 Depinning of a planar cracks

The clearest example of crack depinning is the case of a planar crack front, studied experimentally in references [26–28]: two Plexiglas plates were sandblasted and then glued together in order to create a disordered low toughness plane where the fracture could propagate. Due to the transparency of the material it was then possible to follow the propagation of the crack as it advanced through the plane (see Fig. 1B). The crack front advances in avalanches, as would be expected from a line driven in a disordered medium. The morphology of the crack front was analyzed extensively and the roughness exponent was originally estimated as $\zeta = 0.63$ [26,27]. In reference [29], the authors record crack avalanches by defining their area by looking at the map of the local waiting times. In this way, it was found that the avalanche area distribution is a power law independently on the crack average velocity.

To understand this experiment, we can schematize the crack as a line moving on the xy plane with coordinates $(x, u(x, t))$ [9–12]. An equation of motion for the deformed line position is obtained by computing, from the theory of elasticity, the variations to the stress intensity factor induced by the deformation of the front. In the quasistatic scalar approximation, this is given by [30]

$$K(\{u(x, t)\}) = K_0 \int dx' \frac{u(x', t) - u(x, t)}{(x - x')^2}, \qquad (3)$$

where K_0 is the stress intensity factor for a straight crack. The crack deforms because of the inhomogeneities present in the materials, which give rise to fluctuations in the local toughness $K_c(x, u(x, t))$. These ingredients can be joined together into an equation of motion of the type

$$\Gamma \frac{\partial h}{\partial t} = K_{ext} + K(\{u(x, t)\}) + K_c(x, u(x, t)), \qquad (4)$$

where Γ is a damping term and K_{ext} is the stress intensity factor corresponding to the externally applied stress [9,10,12]. Equation (4) belongs to the general class of interface models. Due to the long-range nature of the

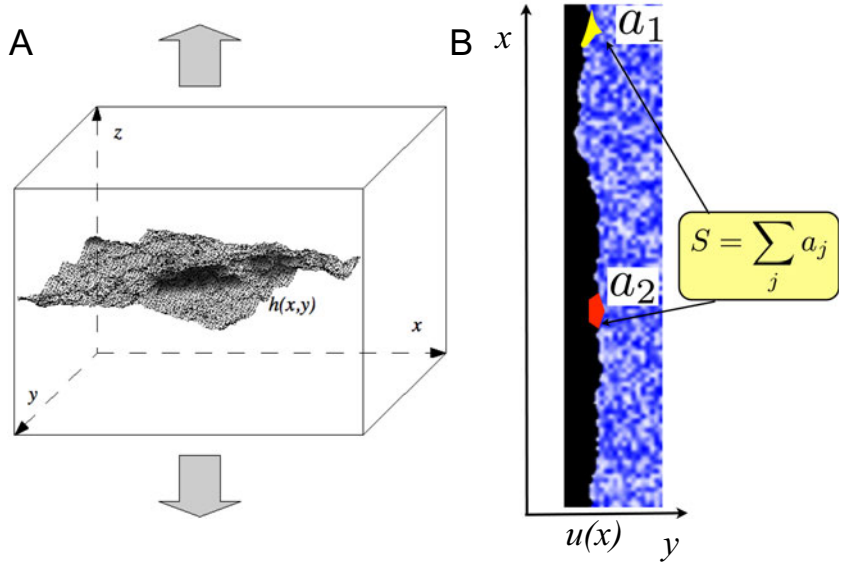

Fig. 1. (A) The geometry of a propagating crack in mode I. The fracture surface is parametrized by a function $u(x, y)$ that displays self-affine scaling. (B) A planar crack seen from above. The front moves in avalanches that are composed by disconnected clusters due to the long-range elastic interactions.

elastic kernel, scaling as $K(q) \sim |q|$ in Fourier space, the theory predicts that the roughness exponent is given by $\zeta \simeq 0.35$ [12,31], which is in disagreement with earlier experiments [26–28], but in agreement with more recent experiments [32] suggesting that the high value of the roughness exponent (i.e. $\zeta = 0.6$) is due to small microcrack coalescence and crosses over to $\zeta = 0.35$ at larger lengthscales.

The validity of equation (4) to describe planar crack front propagation is also confirmed by the statistical analysis of crack avalanches [33,34]. In the original experimental paper [29], avalanches were defined by analyzing the front waiting times. Since the front is always moving, although slowly, an avalanche can be defined as a connected region where the local velocity is above a threshold. Interactions in equation (4) are long-ranged and therefore it can happen that two disconnected regions are casually connected and therefore part of the same dynamical event. One can therefore define an *avalanche* as the region of casually connected events and split it into locally connected *clusters* [34]. It turns out that both avalanches and clusters sizes (s and a) are power law distributed with two different exponents $\tau = 1.25$ and $\tau_a = 1.5$ in agreement with the theoretical predictions [34].

To summarize, experimental measurements of the roughness of planar crack fronts and of more general crack surfaces typically display crossover scaling between large exponents (i.e. $\zeta \simeq 0.6$ or $\zeta_\perp \simeq 0.8$) at small lengthscales and smaller exponents (i.e. $\zeta \simeq \zeta_\perp \simeq 0.3 - 0.4$) at larger lengthscale. There is also indication that multiscaling is present a short lengthscales [32]. The prevalent interpretation of these data considers the large lengthscale exponent as a manifestation of the scaling associated with interface depinning with long-range forces [22,24]. The small scale regime should instead be due to processes that deviate from linear elasticity, but a quantitative theory is still missing.

3 Fracture statistics and size effects

3.1 The problem of fracture size effects

Understanding when materials fracture has been a problem for centuries and more. A crucial issue is the nontrivial dependence of the fracture strength on the characteristic lengthscales of the samples: the fracture size effect. This phenomenon was already noted by Leonardo da Vinci, who measured the carrying-capacity of metal wires of varying length [35]. He observed that the longer the wire, the less weight it could sustain. The reason for this behavior is rooted in the disorder present in the material. The key theoretical concepts needed to understand the problem date back to the pioneering work of Gumbel [36] and Weibull [37] on the statistics of extremes. The general idea stems from a weakest link argument: the failure strength of an extended object is ruled by its weakest local subvolume. For a disordered system, the larger the sample the easiest it is to find a weak region. The Weibull distribution represents still today the main tool used to analyze failure statistics in various materials, although the validity of its underlying assumptions is in general difficult to demonstrate.

Real samples can not generally be schematized as a chain of independent elements with random failure thresholds. In many cases, such as in quasi-brittle materials, the sample does not even fracture at once but sustains a considerable amount of damage before failure. Furthermore, long-range elastic interactions could correlate different regions of the sample invalidating the assumptions used to

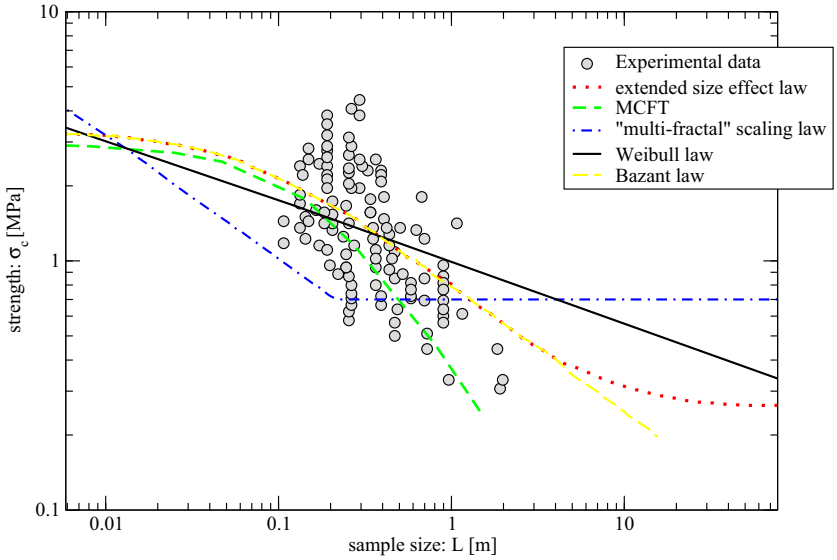

Fig. 2. Size effects measured experimentally in concrete samples. The results can be fitted with a variety of "size-effect laws", but it is difficult to decide if any of those works (adapted from Ref. [40]).

derive the Weibull statistics. The assumption that interactions and microcrack growth would be irrelevant at sufficiently large scales, leading to the recovery of the Weibull distribution, has never been proven rigorously. It would be desirable to relate the failure statistics to some geometrical characteristics of the microstructure of a material, going beyond a simple description of a sample as a collection of regions with different random strengths.

The assumption of independent random damage is hard to justify in quasi-brittle materials, such as concrete and many other composites, where sample failure is preceded by significant damage accumulation and by the formation of large flaws [38]. Failure in quasi-brittle materials is thus determined by the competition between deterministic effects, due to the stress enhancement created by the flaw, and the damage accumulation around the defect due to the stress concentration. The effect of disorder is often treated in an effective medium sense by defining a fracture process zone (FPZ) around the crack tip. Starting from these observations, several theoretical formulations based on linear elastic fracture mechanics (LEFM) have been proposed in the literature and compared with experiments [15,39]. The problem is that the scatter in the experimental data is so great that it is difficult to decide which theory is correct basing the analysis only on the average strength (see Fig. 2) [40]. In addition, one is often interested in extrapolating the results to large scales, relevant for engineering problems, where the theories deviate dramatically one from the other and no experiments are available. Notice also that LEFM is a continuum theory and does not tell us anything about fluctuations. The statistical physics approach offers a possible way to out with the use of simple lattice models, which allow for relatively simple descriptions of disorder and elasticity [41]. The models are sometimes amenable to analytical solutions, and usually are simulated numerically. In the simplest approximation, elastic interactions are replaced by a load transfer rule which is applied when elements fail or get damaged. These fiber bundle models can be solved exactly in some cases [42] and can thus provide a useful guidance for the simulations of more realistic models in which the elastic medium is represented by a network of springs or beams (for a review see Ref. [41]). In this case, the local displacements can then be found by standard methods for solving coupled linear equations. Disorder is modeled by imposing random failure thresholds on each element or by removing a fraction of the links. The lattice is loaded imposing appropriate boundary conditions and the fracture process can be followed step by step, in a series of quasi-equilibria. The simplest and widely used model in past decades has been the random fuse model (RFM) [43], a lattice model for the fracture of solid materials in which as a further key simplification vectorial elasticity has been substituted with a scalar field.

3.2 Extreme value theory

Extreme value theory (EVT) represents the first statistical theory to deal with fracture size effects [36,37,44]. EVT idealizes a random elastic solid as a chain with random failure strengths for each link (see Fig. 3A). The chain is supposed to fail when the external stress is sufficient to break the weakest link. The failure strength distribution is then related to the distribution of the minumum value of a set of random numbers corresponding to the failure strength of each link. In mathematical terms, we consider a series of N elastic links that can sustain at most a stress x_i without breaking. Assuming that the threshold stresses x_i are independent random variables distributed according to a probability density function $p(x_i)$ and cumulative (survival) probability $S(\sigma) \equiv \mathcal{P}(x_i > \sigma) = \int_\sigma^\infty p(x)dx$, the global survival probability $S_N(\sigma)$ for a chain composed

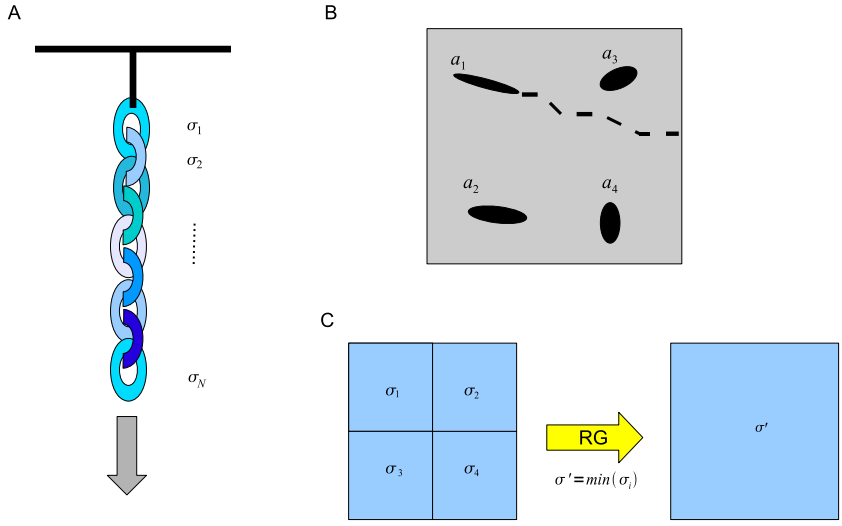

Fig. 3. (A) The weakest link hypothesis. The sample is considered as a chain composed by links of different strength σ_i. The chain fails when the weakest link fails. (B) Nucleation theory. The sample contains a collection of microcracks and the largest one will grow and break the sample. (C) Renormalization group. We can coarse grain the system by subdividing it in four boxes with different strength σ_i. The strength of the large system is chosen to be the minimum of the stresses of the subsystems. If the strengths are independent random variables, by iterating this transformation we recover the results of extreme value theory.

by N links under a stress σ is given by

$$S_N(\sigma) = S(\sigma)^N. \tag{5}$$

In the limit $N \to \infty$, $S_N(\sigma)$ converges to an asymptotic form when stress is properly rescaled

$$S^*(\sigma) = \lim_{N\to\infty} S(A_N\sigma + B_N)^N, \tag{6}$$

where A_N and B_N are appropriate rescaling constants. It is possible to prove that the asymptotic distribution can have only three forms: the Gumbel, the Weibull, and the Fréchet distributions. The Gumbel distribution is given by

$$\Lambda(\sigma) \equiv \exp[-e^{\sigma}], \ \sigma \in \Re, \tag{7}$$

the Weibull distribution is given by

$$\Psi_\alpha(\sigma) \equiv e^{-\sigma^\alpha}, \ \sigma, \alpha > 0, \tag{8}$$

while the Fréchet distribution is not relevant for fracture. The asymptotic behavior of the rescaling constant determines the size effect law. For the Gumbel distribution the typical strength scales as $1/\log(N)$ and for the Weibull distribution as $N^{-1/\alpha}$.

Since the Gumbel distribution is defined also for negative values of σ and failure stresses are obviously only positive, the Weibull distribution is the most commonly used distribution to fit experimental results. Excluding a priori the Gumbel distribution is not really justified: one could argue in the same way that the Gaussian distribution can not be used to fit the sum of positive random numbers since it would allow for a finite probability for negative numbers. As for the Gaussian distribution the convergence to the Gumbel distribution occurs only asymptotically and the contribution of the negative tails vanishes in the limit $N \to \infty$.

3.3 Renormalization group

In statistical physics, the natural framework to investigate large scale properties of interacting system is provided by the renormalization group (RG) theory. Typically, a RG transformation proceeds in two steps: in the first step the system is coarse-grained by eliminating short length-scale degrees of freedom, and then the resulting system is rescaled. The RG coarse-graining for fracture is equivalent to the weakest link hypothesis [45,46]: a system of size L in d dimensions survives at a stress σ if its $n(b) = b^d$ sub-systems of size L/b survive at the same stress (see Fig. 3C). This coarse-graining leads to the following recursion relation for the survival probability

$$S_L(\sigma) = \left[S_{L/b}(\sigma)\right]^{n(b)}. \tag{9}$$

The second step of the RG transformation is to rescale the stress in order to find fixed point distribution S^* that is invariant under RG

$$S^*(\sigma) = \mathcal{R}[S^*(\sigma)] \equiv [S^*(A\sigma + B)]^{n(b)}. \tag{10}$$

Clearly repeated iteration of the RG transformation leads to the same results as the asymptotic limit of EVT, but the RG framework could be useful to better understand the role of elastic interactions. The EVT fixed point is derived assuming that no interactions are present: failure stresses are considered as independent random variables. If the theory is correct then elastic interaction should be irrelevant at large length scales. Recent large scale numerical simulations of the RFM indicate that indeed this is the case at least for weak disorder [47].

3.4 Nucleation theory

EVT theory describes the asymptotic properties of the failure probability distribution, but its convergence can be quite slow on the low probability tails [47]. On the other hand, it is sometimes of great importance to evaluate the failure probability at low stresses. To this end, one can use an analogy with nucleation theory and compute the stress required to turn unstable the least stable crack in the system [48–51]. The energy associated with a linear crack of length a under a far-field stress σ in two dimensions is given by

$$\mathcal{E} = -\frac{\pi\sigma^2 a^2}{2E} + 2aG_f, \tag{11}$$

where E is the Young modulus and G_f is the fracture toughness. The first term is the elastic energy released by the crack and the second term is the surface energy needed to separate the crack surfaces apart. As in nucleation theory, we have a competition between a bulk and a surface term leading small cracks to shrink and large cracks to grow. The boundary between these two regimes is controlled by the applied stress so that a crack length a becomes unstable at a stress

$$\sigma = \sqrt{\frac{2EG_f}{\pi a}}. \tag{12}$$

Now consider an area L^2 with a set of independent random cracks whose lengths are distributed according to given probability density function $p(a)$ and cumulative distribution $P(a)$ (see Fig. 3B). The probability distribution that the largest crack is larger than a is given by EVT

$$P_N(a) \simeq 1 - \exp[-\rho V P(a)], \tag{13}$$

where $\rho \equiv N/L^2$. For an exponential crack distribution, equation (13) becomes a Gumbel distribution [36]

$$P_N(a) = 1 - \exp[-\rho V \exp(-a/a_c)], \tag{14}$$

where a_c is the characteristic scale of the crack length distribution. Combining equations (14) and (12), one can derive the survival distribution as

$$S_L(\sigma) \simeq 1 - e^{-\rho L^2 \exp(\frac{\sigma_0}{\sigma})^2}, \tag{15}$$

where $\sigma_0^2 \equiv 2EG_f/\pi a_c$, known as the Duxbury-Leath-Beale (DLB) distribution [51], which is not an asymptotic distribution of EVT, converging eventually to the Gumbel distribution [47].

Large scale simulations of the RFM with a pre-existing exponential crack distribution indicate that the survival distribution is indeed well represented by the DLB distribution [47]. This suggests that the asymptotic distribution for fracture of weakly disordered media is the Gumbel distribution. This observation may have little practical relevance since convergence is extremely slow and for finite systems the Gumbel distribution does a bad job in fitting the distribution tails. The general validity of the DLB distribution for fracture is intriguing issue that needs to be confirmed for different kind of disorders and loading conditions.

3.5 Size effects in notched samples

A very common experimental setting to study size effects involves a specimen containing a pre-existing notch. Failure in this case is determined by the competition between the deterministic stress enhancement at the tip of the notch and a random contribution due to structural disorder [52]. For large notches disorder is considered a small perturbation, defining a FPZ around the crack tip, where all the damage is confined (see Fig. 4A). For quasi-brittle materials, however, the size of the FPZ may not be negligible when compared to the system size and the problem may become subtle.

As discussed above, the standard approach based on LEFM considers the stability of the notch against failure is given by the Griffith's criterion for the critical stress (see Eq. (12)). A scaling law for the size-effect has been proposed by Bazant for quasi-brittle materials [15], introducing in the Griffith expression an additional length-scale ξ due to the presence of a FPZ

$$\sigma = K_c/\sqrt{\xi + a_0}, \tag{16}$$

where a_0 is the linear size of the notch and $K_c \sim \sqrt{EG_f}$ is the critical stress intensity factor. Equation (16) implies that in the large notch limit $\xi/a_0 \ll 0$ one recovers LEFM scaling, in which the strength is inversely proportional to $1/\sqrt{a_0}$, while for a vanishing external flaw size $a_0 \to 0$, the average strength remains finite.

Using numerical simulations of disordered fracture models, such as the random fuse model [53] or more complex bond or beam model [54], it was possible to check the validity of equation (16) in controlled conditions. These simulations show that equation (16) is correct for large notches and allows to connect the lengthscale ξ with the size of damage pattern ahead of the notch (see Fig. 4B). For small notch sizes, however, the law crosses over to a size dependent form ruled by EVT. The cross-over takes place at a scale a_c which can be obtained equating the strength prediction of equation (16) and the scaling of a sample without a notch $\sigma_0(L, D)$ (see Fig. 4C). One can condense these results into a single scaling theory, valid for all a_0, stating that

$$\frac{K_c^2}{\sigma^2} = \xi + a_0 f(a_c/a_0) \tag{17}$$

where the statistical scaling function $f(y)$ is characterized by

$$f(y) \simeq \begin{cases} 1 & \text{if} \quad y \ll 1 \\ y & \text{if} \quad y \gg 1 \end{cases} \tag{18}$$

and the cross-over scale is given by

$$a_c \simeq (K_c(D)/\sigma_0(L, D))^2 - \xi(D). \tag{19}$$

3.6 Fracture of fractal media

A large effort in the literature has been devoted to understand the relation between the crack morphology or the

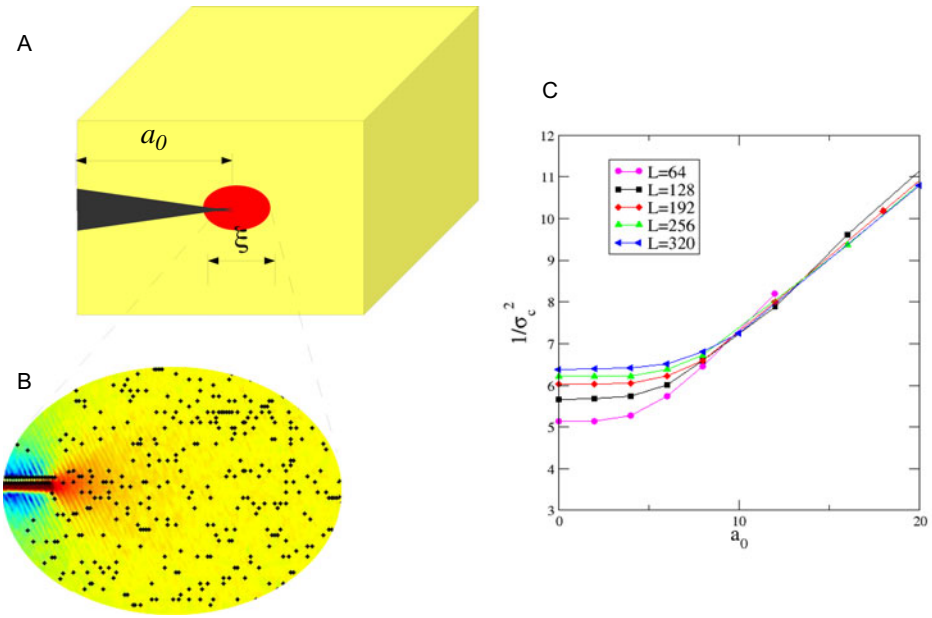

Fig. 4. (A) In quasi-brittle materials the length of the notch a_0 is correcred by the size of the fracture process zone ξ. (B) The fracture process zone can be revealed in simulations of the random fuse model by averaging over disorder (see Ref. [53]). (C) The size effect law predicted by linear-elastic fracture mechanics is corrected by disorder. The results are from simulations of the random fuse model reported in reference [53].

material microstructure and the resulting size effects. As discussed above, crack fronts exhibit a self-affine structure and it has been attempted to use this property to derive the size dependence of the strength [55]. A popular argument interprets size effects as the result of internal fractal structure of the material [56,57] leading to heated debates on its validity in the engineering community [40]. While no material is fractal on long lengthscales, it would be still be interesting to characterize more rigorously the scale dependence of the failure properties of general fractal objects. To this end, however, one should abandon the appealing but misleading idea of a continuum mechanics on fractals and work instead with a discrete system.

The mechanics of a fractal cannot be treated by replacing the Euclidian dimension with the fractal dimension in the relevant equation. This can be understood by a simple example: in homogeneous materials the stress is defined by the total applied force F divided by the section $S \sim L^2$, where L is the linear size of the sample, and scales $\sigma \sim F/L^2$. Now consider a fractal material with fractal dimension D, whose section would scale as $S \sim L^{D-1}$. One could argue that the real internal stress should now scale as $\sigma \sim F/L^{D-1}$ and predict a power law size effect in terms of the nominal applied stress [56]. Stress in a fractal, however, is carried only by a limited number of bonds that is not directly related to the fractal dimension. To disconnect the fractal percolation cluster for instance it is enough to break one "red" bond, rather than a number of bonds scaling as L^{D-1}.

Many size effect fractal theories rely on the idea that if the crack surface is fractal then the scaling of the stress needed to create it should derive from its morphology [56]. As we discussed above, fracture surfaces are not self-similar but self-affine and ignoring this fact leads to spurious results as discussed in reference [58]. Apart from this, the general argument is still questionable: failure usually occurs when a crack becomes unstable and grows. The stress causing failure in principle does not know about the future path taken by the crack in its dynamics. So it is not obvious that there is any relation between the morphology of the fracture surface and the stress needed to create it. This is supported by numerical simulations of disordered fracture models, where the failure strength and the related size effects are not related with the final self-affine crack geometry but rather with the exponential distribution of crack sizes observed at peak load [47].

4 Strain bursts and size effects in microplasticity

4.1 The challenges of microplasticty

Plastic deformation is a paradigmatic problem of multiscale materials modeling. Relevant processes range from the small scales where atomic arrangements are of crucial importance for its deformation properties, up to macroscopic scales where deformation instabilities manifest themselves in the form of catastrophic failure. The crucial question of how defect and microstructural properties link to the macroscopic constitutive equations of continuum mechanics is still not completely answered. Very often it has been assumed that the transition from discrete defects and microstructural features to continuum mechanics can be accomplished by studying single defect

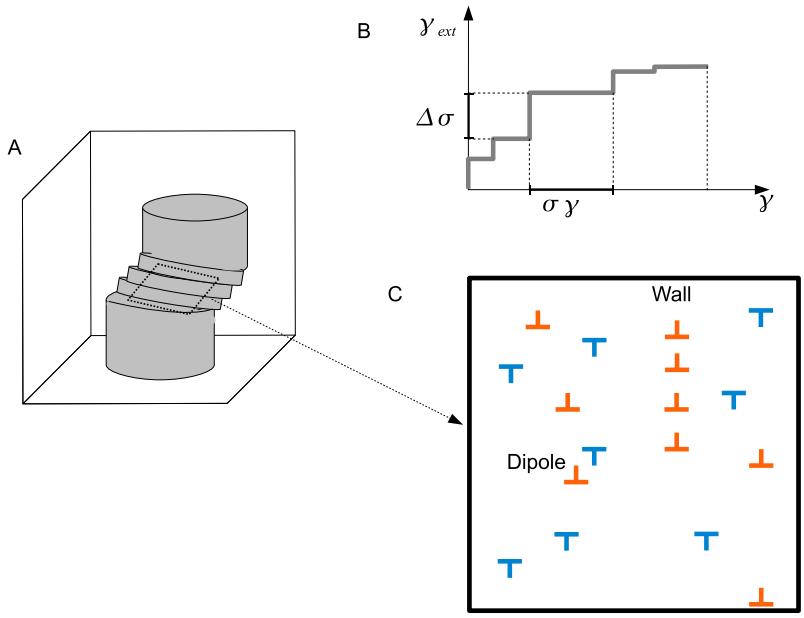

Fig. 5. (A) Micron-scale sample deform irreversibly with large plastic strain bursts that can be seen from the sample surface. (B) The stress-strain curve has a staircase-like character with random stress and strain jumps. (C) The simplest model for micron-scale plasticity considers a cross section of the sample populated by gliding edge dislocations with positive and negative burgers vectors. Strain bursts are due to the breakup of blocked configurations such as walls or dipoles.

models or by performing simple homogenization procedures – as soon as one is well above the scale of the relevant defects, straightforward averaging of their individual dynamics should lead to the smooth laws envisaged by continuum mechanics. This conventional viewpoint has been recently challenged by experiments investigating deformation fluctuations under conditions where plastic deformation was expected to occur in a smooth and stable manner. For instance, in plastically deformed micron-sized crystals, internal dislocation avalanches lead to jumps in the stress-strain curves (strain bursts) whereas in macroscopic samples plasticity appears as a smooth process (see Fig. 5) [59]. In addition, the deformation tests reveal intriguing size effects: the plastic yield stress is found to increase as the sample size is decreased [2]. The generality of this result is confirmed by compression tests on micropillars fabricated from a variety of materials with different crystal lattice structures, including Ni [2,60,61], Au [62,63], Cu [64], Mo [65,66], and LiF [67], supporting the now popular paradigm that smaller is stronger [2]. Notice that size effects are not observed in macroscopic samples that are thus well described by continuum mechanics. Strain burst are indirectly revealed also in macroscopic samples by acoustic emission measurements [68–70] although the deformation curves are apparently smooth [71]. In the materials science literature there is still, however, no consensus on the mechanisms underlying size effects and strain bursts in micropillars, although several theoretical arguments have been proposed. Some theories are based on statistical effects [72–74] while others emphasize the role of sample boundaries and dislocation sources [62,63]. Despite these interesting developments, a quantitative theory explaining the scaling of the strength and the strain bursts is still lacking.

4.2 Discrete dislocation dynamics simulations: two dimensions

Several interesting features of microplasticity can be reproduced by discrete dislocation dynamics (DDD) simulations, in which one follows the dynamics of an ensemble of interacting dislocations. The simplest DDD model can be thought to represent the cross section of a single-slip oriented crystal where N point-like edge dislocations glide in the xy plane along directions parallel to the x axis (see Fig. 5C). Dislocations with positive and negative Burgers vectors $\mathbf{b}_n = \pm b\hat{x}$ are assumed to be present in equal numbers, and the initial number of dislocations is the same in every realization. An edge dislocation with Burgers vector $b\hat{x}$ located at the origin interacts by a long-range force with a dislocation in $\mathbf{r} = (x, y)$. Assuming an overdamped dynamics, in which the dislocation velocities are linearly proportional to the local forces, the velocity of the nth dislocation along the glide direction

$$\chi v_n = b_n \left[\sigma_e + \sum_{m \neq n} \sigma_{xy}(\mathbf{r}_{nm}) \right], \tag{20}$$

where χ is the damping constant,σ_e is the external stress, $\mathbf{r}_{nm} \equiv \boldsymbol{r}_n - \boldsymbol{r}_m$ the relative position vector of dislocations n and m, and the the relevant component of the shear stress for edge dislocations is given by

$$\sigma_{xy}(\mathbf{r}) = \frac{Gb}{2\pi(1-\nu)} \frac{\cos\theta \cos 2\theta}{r}, \tag{21}$$

where G is the shear modulus and ν the Poisson ratio. Periodic boundary conditions are usually imposed in the direction of motion (i.e. the x axis) but often along both

directions. In order to take correctly into account the long range nature of the elastic interactions, the stress should be summed over an infinite number of images. When the distance between two dislocations is of the order of a few Burgers vectors, linear elasticity theory breaks down. In these instances, phenomenological nonlinear reactions, such as the annihilation of a pair of dislocations, describe more accurately the real behavior of dislocations in a crystal. Typicall, one *annihilates* a pair of dislocations with opposite Burgers vectors when the distance between them is shorter than a cutoff y_e [69,75].

The dynamics of interacting dislocations displays interesting glassy relaxation properties [75–78]. The strain rate initially decays as a power law but at larger times it crosses over to a linear creep regime (i.e. to a plateau signaling a steady rate of plastic deformation) whenever the applied stress is larger than a critical threshold σ_c, or, otherwise, to decay exponentially to zero [75]. These results suggested that a possible interpretation of dislocation dynamics in terms of the general *jamming* framework proposed to encompass a wide variety of non-equilibrium soft and glassy materials [79]. Most of these physical systems consist of various types of soft particles closely packed into an amorphous state. At high densities, the relative motion of these particles is drastically constrained and, as a consequence, soft and concentrated materials usually respond like elastic solids upon the application of low stresses. One then says that the system is jammed, since it is unable to explore all the available configuration space. On the other hand, they flow like viscous fluids above a yield stress value σ_y.

The particle density is usually a control parameter in the jamming transition, but not for dislocations. Equations (20) and (21) are invariant if we rescale all lengths in proportion with the mean dislocation spacing $1/\sqrt{\rho}$, all times in proportion with $1/\rho$, and the externally applied stress in proportion with $\sqrt{\rho}$ [80,81]. Hence if a set of dislocations with density ρ_0 is jammed at a stress below σ_0, then a set with dislocation with density ρ will be jammed below $\sigma_c = \sqrt{\rho/\rho_0}\sigma_0$. In other words, contrary to other jamming systems dislocations should jam at all densities [82]. An exception to this rule may come from the fact that the critical stress vanishes: Recent numerical simulations explored the variation of the critical stress with system size and provided preliminary indications that it may indeed decrease to zero as the number of dislocations diverge [78]. Further work is needed to clarify this issue.

4.3 Discrete dislocation dynamics simulations: three dimensions

DDD simulations reveal dislocation avalanches with a power law distribution of energies due to the breakup of jammed configurations [69]. In two dimensions, these metastable configurations are essentially walls or dipoles. Avalanches in more realistic configurations can be obtained in three dimensional dislocation dynamics simulations [83–85]. These kind of models are extremely challenging from the computational point of view and for this reason one has access only to relatively small sample sizes. On the other hand, they provide a more faithful representation of the dynamics of interacting dislocations, including the formation of junctions, the multiplication of dislocation through Franck-Read sources and the effect of the boundary conditions on the elastic stresses. The scaling features of the avalanches distribution persist in three dimensions, with an exponent $\tau \simeq 1.5$. In addition, the exponent is the same for single slip and multiple slip, does not depend on the presence of cross-slip and on the loading mode. The value of the cutoff to the power law distribution changes with the loading mode [83]. The robustness of the exponent value is supported by the agreement between experiments and model. In addition, the value is very close to the typical mean-field prediction $\tau = 3/2$. Under the guidance of the numerical simulations, it is possible to obtain the scaling of the cutoff of the avalanche distribution, given by

$$s_0 = \frac{bE}{L(\Theta + \Gamma)}, \tag{22}$$

where E is the Young modulus, L is the linear size of the system, Θ is the hardening coefficient and Γ is the stiffness of the traction machine when the sample is loaded under strain control [83]. Using this expression it is possible to collapse all the simulated and experimental distribution into a single master curve [83]. This general scaling law was later confirmed by other independent three dimensional dislocation dynamics simulations [84] and by experiments in Mo and Au micropillars [65].

These findings have important implications for deformation processes on the micron scale. As a consequence of the stochastic and intermittent nature of the deformation process, the deformation behavior of a small enough sample can no longer be predicted in a deterministic sense. As the maximum avalanche strain increases with decreasing system size, the stochastic heterogeneity of deformation becomes more and more pronounced, Hence it may be difficult, on the micron and sub-micron scale, to control the results of plastic forming processes. This problem could be relevant in the processing of micron-scale components such as bonding wires in chips.

4.4 Yielding and depinning

The analysis reported in the previous sections shows that there are intriguing analogies the dynamics of an assembly of interacting dislocation moving on different glide planes and the depinning of elastic manifolds in disordered media. This analogy has been reformulated into a more rigorous framework by Zaiser and Moretti [86], employing the formalism of continuum plasticity. They consider a single slip system (along the x direction) and describe the plastic strain by a field $\gamma((r))$, assuming it is independent of the z coordinate. These conditions closely represent the geometry of the dislocation dynamics model discussed above. Employing a general viscoplastic constitutive law, one can write

$$\frac{\partial \gamma}{\partial t} = C[\sigma_e + \sigma_{int}(r,\gamma) + \sigma_p(r,\gamma)], \tag{23}$$

where σ_e is the externally applied stress and σ_p is the effective pinning stress due to immobile threading dislocations or by solute atoms. The internal stress induced by the local fluctuations of the strain field $\gamma(\mathbf{r})$ can be computed in the framework of linear elasticity. In Fourier space, it is given by $\tilde{\sigma}_{int} \propto \tilde{\gamma}_{\mathbf{k}} k_x^2 k_y^2/|k|^4$. Equation (23) is this equivalent to the one describing an elastic manifold with non-local stiffness moving in a disordered landscape under the action of an external force. In this sense, we can explain the occurrence of avalanches in crystal plasticity as the signature of a *yielding* transition, which in the particular case considered here can be mapped into a depinning transition. If this mapping is correct, a size effect would stem naturally from finite size scaling as in other depinning transitions [87]. Namely the depinning stress in a finite systems should scale as

$$\sigma_c(L) = \sigma_c(\infty) + A/L^{1/\nu_{FS}} \tag{24}$$

where ν_{FS} is the finite size scaling exponent [87].

Finally, it is important to emphasize here the crucial role played by work hardening in the yielding transition. In most materials dislocation proliferation effectively increases the stress necessary to sustain dislocation motion. This effect is usually modeled by increasing the flow stress or equivalent by introducing an additional back-stress $\sigma_B = -\Theta\gamma$, where Θ is the hardening coefficient. Thus if we ramp up the external stress the back stress keeps the effective stress $\sigma_e + \sigma_B$ close to the critical yield stress, introducing a cutoff in the avalanche distribution that is controlled by Θ [83,88]. While we can expect that the yielding transition represents a useful theoretical framework to understand plastic flow in general, the detailed implementation of the program for a generic multiple slip system of interacting curved dislocation appears to lie well beyond the present possibilities.

4.5 Amorphous plasticity

Strain burst and size effects are not restricted to crystal micro-plasticity: compression of amorphous micro-pillars yields very similar phenomenology [89]. Atomistic simulations of plastically deformed amorphous materials have shown intermittent strain bursts similar to those observed in crystal plasticity [90–93]. In amorphous materials such as glasses, pastes or foams, in the absence of an underlying crystalline lattice, plasticity cannot be described in terms of dislocations. It is usually assumed, however, that macroscopic deformation can be considered as a succession of localized reorganizations at some microscopic scale [94]. These rearrangements give rise to quadrupolar stress redistributions that are analogous to those occurring when a dislocation slips forward by one lattice step. It is interesting to notice that models very similar to equation (23) have been used to described amorphous plasticity [95,96]. It is therefore conceivable that universality in plastic strain avalanches may exist for crystals and amorphous materials.

From a mesoscopic perspective the yield surface of an amorphous material results from the joint optimization of local intrinsic disorder and elasticity. Based on a powerful analogy, it has been suggested that strain localization in the perfect plasticity (PP) limit can be related to the problem of finding the minimum energy (ME) surface in a disordered medium [97]. This is a generic optimization problem in disordered media in which one searches for the path that minimizes the sum of a given local random variable that is called energy. The conjectured equivalence between PP and ME comes from the observation that, at the yield point, it is not possible to find an elastic path, along which the stress could increase, spanning the sample from end to end. Recently, it has shown [98] that PP and ME are not exactly the same but the universality class of the problem is the same. In particular, the size effects and the yield stress distribution are very similar [98,99]. These models are very simplified and whether similar optimization induced scaling can explain real size effects remains to be tested.

5 Outlook

In this colloquium I have tried to highlight some general problems in fracture and plasticity where a statistical physics approach lead to promising results and improved understanding. The past decades have witnessed an increasing numbers of contributions in this field and it is difficult to review all the relevant literature. I therefore focused on three problems that have benefited in the past by statistical mechanics methods and still present several intriguing unresolved issues.

Thanks to the development of refined theories for interface depinning and detailed experiments on a variety of materials, we now understand the roughness of fracture surfaces much better than three decades ago, when their self-affine nature was first revealed. Yet, some aspects of the problem still remain to be elucidated. For instance, we still do not have a quantitative theory for the short-length scale fracture regime where one observes multi-scaling.

Understanding size effects and strength distributions is one of the key problems in fracture that has been studied by statistical methods for more than a century. Improvement in computational power now allow for large scale numerical simulations of disordered fracture models with impressive statistical sampling. This will allow more and more to discriminate between different statistical theories and guide the establishment of more reliable safety factors for large structures.

Finally, in the last decade there has been a flurry of activity in micron-scale plasticity. This is becoming a very important field with relevance for future microtechnologies. Statistical physics thinking is more and more useful to interpret the huge amount of experimental and numerical simulations data.

In conclusions, the mechanics of materials represents an extremely exciting playground for statistical physicists. In this colloquium, I have discussed a few examples but more problems exist and wait to be explored.

The ideas reported in this colloquium are largely the result of extensive discussions and collaborations with many colleagues to which I express my gratitude. In particular I wish to thank M.J. Alava, L. Laurson, J.M. Lopez, C. Manzato, M.-C. Miguel, P.K.V.V. Nukala, C. Picallo, J.P. Sethna, A. Shekhawat and M. Zaiser. This work is supported by the European Research Council, AdG2011-SIZEFFECTS.

References

1. M.J. Alava, P.K.V.V. Nukala, S. Zapperi, J. Phys. D **42**, 214012 (2009)
2. M.D. Uchic, D.M. Dimiduk, J.N. Florando, W.D. Nix, Science **305**, 986 (2004)
3. D.M. Dimiduk, C. Woodward, R. Lesar, M.D. Uchic, Science **312**, 1188 (2006)
4. J.R. Greer, J.T.D. Hosson, Progr. Mater. Sci. **56**, 654 (2011), festschrift Vaclav Vitek
5. M.D. Uchic, P.A. Shade, D. Dimiduk, Annu. Rev. Mater. Res. **39**, (2009)
6. O. Kraft, P.A. Gruber, R. Mönig, D. Weygand, Annu. Rev. Mater. Res. **40**, 293 (2010)
7. D. Fisher, Phys. Rep. **301**, 113 (1998)
8. M. Kardar, Phys. Rep. **301**, 85 (1998)
9. J. Schmittbuhl, S. Roux, J.P. Villotte, K.J. Maloy, Phys. Rev. Lett. **74**, 1787 (1995)
10. S. Ramanathan, D.S. Fisher, Phys. Rev. Lett. **79**, 877 (1997)
11. S. Ramanathan, D. Ertas, D.S. Fisher, Phys. Rev. Lett. **79**, 873 (1997)
12. S. Ramanathan, D.S. Fisher, Phys. Rev. B **58**, 6026 (1998)
13. S. Zapperi, M. Zaiser, Mater. Sci. Eng. A **309-310**, 348 (2001)
14. P. Moretti, C.M. Miguel, M. Zaiser, S. Zapperi, Phys. Rev. B **69**, (2004)
15. Z.P. Bazant, Proc. Natl. Acad. Sci. USA **101**, 13400 (2004)
16. B.B. Mandelbrot, D.E. Passoja, A.J. Paullay, Nature **308**, 721 (1984)
17. E. Bouchaud, J. Phys.: Condens. Matter **9**, 4319 (1997)
18. D. Bonamy, E. Bouchaud, Phys. Rep. **498**, 1 (2011)
19. E. Bouchaud, G. Lapasset, J. Planès, S. Naveos, Phys. Rev. B **48**, 2917 (1993)
20. P. Daguier, B. Nghiem, E. Bouchaud, F. Creuzet, Phys. Rev. Lett. **78**, 1062 (1997)
21. Y.B.J. Schmittbuhl, S. Roux, Europhys. Lett. **28**, (1994)
22. L. Ponson, D. Bonamy, E. Bouchaud, Phys. Rev. Lett. **96**, 035506 (2006)
23. J.M. Boffa, C. Allain, J. Hulin, Eur. Phys. J. AP **2**, 281 (1998)
24. D. Bonamy, L. Ponson, S. Prades, E. Bouchaud, C. Guillot, Phys. Rev. Lett. **97**, 135504 (2006)
25. J.P. Bouchaud, E. Bouchaud, G. Lapasset, J. Planès, Phys. Rev. Lett. **71**, 2240 (1993)
26. J. Schmittbuhl, K.J. Maloy, Phys. Rev. Lett. **78**, 3888 (1997)
27. A. Delaplace, J. Schmittbuhl, K.J. Maloy, Phys. Rev. E **60**, 1337 (1999)
28. K.J. Maloy, J. Schmittbuhl, Phys. Rev. Lett. **87**, 105502 (2001)
29. K.J. Maloy, S. Santucci, J. Schmittbuhl, R. Toussaint, Phys. Rev. Lett. **96**, 045501 (2006)
30. H. Gao, J.R. Rice, J. Appl. Mech. **56**, 828 (1989)
31. D. Ertas, M. Kardar, Phys. Rev. E **49**, R2532 (1994)
32. S. Santucci, M. Grob, R. Toussaint, J. Schmittbuhl, A. Hansen, K.J. Maly, Europhys. Lett. **92**, 44001 (2010)
33. D. Bonamy, S. Santucci, L. Ponson, Phys. Rev. Lett. **101**, 045501 (4) (2008)
34. L. Laurson, S. Santucci, S. Zapperi, Phys. Rev. E **81**, 046116 (2010)
35. L. da Vinci, *I Libri di Meccanica* (Hoepli, Milano, 1940)
36. E.J. Gumbel, *Statistics of Extremes* (Columbia University Press, New York, 2004)
37. W. Weibull, *A Statistical Theory of the Strength of Materials* (Stockholm, 1939)
38. J.G.M. van Mier, *Fracture Processes of Concrete* (CRC Press, Boca Raton, USA, 1996)
39. X.Z. Hu, F. Wittmann, Mater. Struct. **25**, 319 (1992)
40. Z.P. Bazant, A. Yavari, Eng. Fract. Mech. **72**, 1 (2005)
41. M.J. Alava, P. Nukala, S. Zapperi, Adv. Phys. **55**, 349 (2006)
42. S.L. Phoenix, I.J. Beyerlein, Phys. Rev. E **62**, 1622 (2000)
43. L. de Arcangelis, S. Redner, H.J. Herrmann, J. Phys. Lett. **46**, 585 (1985)
44. F.T. Pierce, J. Textile Inst. **17**, 355 (1926)
45. G. Györgyi, N.R. Moloney, K. Ozogány, Z. Rácz, Phys. Rev. Lett. **100**, 210601 (2008)
46. G. Györgyi, N.R. Moloney, K. Ozogány, Z. Rácz, M. Droz, Phys. Rev. E **81**, 041135 (2010)
47. C. Manzato, A. Shekhawat, P.K.V.V. Nukala, M.J. Alava, J.P. Sethna, S. Zapperi, Phys. Rev. Lett. **108**, 065504 (2012)
48. A.M. Freudenthal, in *Fracture*, edited by H. Liebowitz (Academic, New York, 1968), p. 591
49. B.K. Chakrabarti, L.G. Benguigui, *Statistical Physics of Fracture and Breakdown in Disordered Systems* (Oxford Science Publications, Oxford, 1997)
50. P.M. Duxbury, P.D. Beale, P.L. Leath, Phys. Rev. Lett. **57**, 1052 (1986)
51. P.M. Duxbury, P.L. Leath, P.D. Beale, Phys. Rev. B **36**, 367 (1987)
52. Z.P. Bazant, J. Planas, *Fracture and Size Effect in Concrete and Other Quasibrittle Materials* (CRC Press, Boca Raton, USA, 1997)
53. M.J. Alava, P. Nukala, S. Zapperi, Phys. Rev. Lett. **100**, 055502 (2008)
54. M. Alava, P. Nukala, S. Zapperi, Int. J. Fract. **154**, 51 (2008)
55. S. Morel, J. Schmittbuhl, E. Bouchaud, G. Valentin, Phys. Rev. Lett. **85**, 1678 (2000)
56. A. Carpinteri, Int. J. Solids Struct. **31**, 291 (1994)
57. A. Carpinteri, Mech. Mater. **18**, 89 (1994)
58. J. Weiss, Int. J. Fract. **109**, 365 (2001)
59. D. Dimiduk, M. Koslowski, R. Lesar, Scr. Mater. **54**, 701 (2006)
60. C. Frick, B. Clark, S. Orso, A. Schneider, E. Arzt, Mater. Sci. Eng. **489**, 319 (2008)
61. C.A. Volkert, E.T. Lilleodden, J. Phil. Mag. **86**, 5567 (2006)
62. J.R. Greer, W.C. Oliver, W.D. Nix, Acta Mater. **53**, 1821 (2005)
63. J.R. Greer, Rev. Adv. Mater. Sci. **13**, 59 (2006)
64. D. Kiener, C. Motz, T. Schöberl, M. Jenko, G. Dehm, Adv. Eng. Mater. **8**, 1119 (2006)
65. J. Greer, C. Weinberger, W. Cai, Mater. Sci. Eng. **493**, 21 (2008)

66. S. Brinckmann, J.Y. Kim, J.R. Greer, Phys. Rev. Lett. **100**, 155502 (2008)
67. E.M. Nadgorny, D. Dimiduk, M.D. Uchic, J. Mater. Res. **23**, 2829 (2008)
68. J. Weiss, J.R. Grasso, J. Phys. Chem. B **101**, 6113 (1997)
69. Miguel, A. Vespignani, S. Zapperi, J. Weiss, J.R. Grasso, Nature **410**, 667 (2001)
70. T. Richeton, J. Weiss, F. Louchet, Nat. Mater. **4**, 465 (2005)
71. J. Weiss, T. Richeton, F. Louchet, F. Chmelik, P. Dobron, D. Entemeyer, M. Lebyodkin, T. Lebedkina, C. Fressengeas, R.J. Mcdonald, Phys. Rev. B **76**, 224110+ (2007)
72. D.M. Norfleet, D.M. Dimiduk, S.J. Polasik, M.D. Uchic, M.J. Mills, Acta Mater. **13**, 2988 (2008)
73. S.I. Rao et al., J. Phil. Mag. **87**, 4777 (2007)
74. S. Rao, D. Dimiduk, T. Parthasarathy, M. Uchic, M. Tang, C. Woodward, Acta Mater. **56**, 3245 (2008)
75. M.C. Miguel, A. Vespignani, M. Zaiser, S. Zapperi, Phys. Rev. Lett. **89**, 165501 (2002)
76. B. Bakó, I. Groma, G. Györgyi, G.T. Zimányi, Phys. Rev. Lett. **98**, 075701 (2007)
77. L. Laurson, M.C. Miguel, M.J. Alava, Phys. Rev. Lett. **105**, 015501 (2010)
78. P.D. Ispánovity, I. Groma, G. Györgyi, P. Szabó, W. Hoffelner, Phys. Rev. Lett. **107**, 085506 (2011)
79. A.J. Liu, S.R. Nagel, Nature **396**, 21 (1998)
80. M. Zaiser, M.C. Miguel, I. Groma, Phys. Rev. B **64**, 224102 (2001)
81. I. Groma, G. Gyorgyi, P.D. Ispanovity, Phys. Rev. Lett. **108**, 269601 (2012)
82. G. Tsekenis, N. Goldenfeld, K.A. Dahmen, Phys. Rev. Lett. **106**, 105501 (2011)
83. F.F. Csikor, C. Motz, D. Weygand, M. Zaiser, S. Zapperi, Science **318**, 251 (2007)
84. B. Devincre, T. Hoc, L. Kubin, Science **320**, 1745 (2008)
85. J. Senger, D. Weygand, P. Gumbsch, O. Kraft, Scr. Mater. **58**, 587 (2008)
86. M. Zaiser, P. Moretti, J. Stat. Mech. **2005**, P08004+ (2005)
87. C.J. Bolech, A. Rosso, Phys. Rev. Lett. **93**, 125701 (2004)
88. M. Zaiser, Adv. Phys. **55**, 185 (2006)
89. Z.W. Shan, J. Li, Y.Q. Cheng, A.M. Minor, S.S.A. Asif, O.L. Warren, E. Ma, Phys. Rev. B **77**, (2008)
90. C. Maloney, A. Lemaître, Phys. Rev. Lett. **93**, 016001 (2004)
91. M.J. Demkowicz, A.S. Argon, Phys. Rev. B **72**, 245206 (2005)
92. C.E. Maloney, A. Lemaître, Phys. Rev. E **74**, 016118 (2006)
93. N.P. Bailey, J. Schiøtz, A. Lemaître, K.W. Jacobsen, Phys. Rev. Lett. **98**, 095501 (2007)
94. M.L. Falk, J.S. Langer, Phys. Rev. E **57**, 7192 (1998)
95. J.C. Baret, D. Vandembroucq, S. Roux, Phys. Rev. Lett. **89**, 195506 (2002)
96. M. Talamali, V. Petäjä, D. Vandembroucq, S. Roux, Phys. Rev. E **84**, 016115 (2011)
97. S. Roux, A. Hansen, J. Phys. II France **2**, 1007 (1992)
98. C.B. Picallo, J.M. López, S. Zapperi, M.J. Alava, Phys. Rev. Lett. **103**, 225502 (2009)
99. C.B. Picallo, J.M. López, S. Zapperi, M.J. Alava, Phys. Rev. Lett. **105**, 155502 (2010)